High-speed wind-tunnel investigation of major aerodynamic challenges for HLFC technology

Fabien Méry, Jean-Luc Godard, Guillaume Arnoult, Philippe Bardoux, Christophe François, Maxime Forte, Estelle Piot

56th 3AF International Conference on Applied Aerodynamics
28 – 30 March 2022, Toulouse - France

FP59-AERO2022-mery

HIGH-SPEED WIND-TUNNEL INVESTIGATION OF MAJOR AERODYNAMIC CHALLENGES FOR HLFC TECHNOLOGY

Fabien Méry[(1)], Jean-Luc Godard[(2)], Guillaume Arnoult[(2)], Philippe Bardoux[(2)] , Christophe François[(2)] , Maxime Forte[(1)] and Estelle Piot[(1)]
[(1)] *ONERA/DMPE, Université de Toulouse, F-31055 Toulouse, France*
[(2)] *DAAA, ONERA, Université Paris Saclay, F-92190 Meudon, France*
Corresponding author: fabien.mery@onera.fr

ABSTRACT

Reduction of the specific consumption of aircraft would lead to substantial economic and environmental benefits. A promising technique consists in reducing skin friction drag by delaying the laminar-turbulent transition point as far aft as possible, particularly on the wings, in order to obtain lower friction coefficient in the presence of laminar flow. This can be achieved by Hybrid Laminar Flow Control (HLFC) technology.
This paper presents the aerodynamic design of a large-scale HLFC wing model for experiments that will be conducted in ONERA's S1MA wind-tunnel. The wing model is designed to investigate the major aerodynamic challenges that must be tackled to enable the development of HLFC airfoils: assessment in transonic flow conditions of the wing drag reduction due to HLFC suction, surface tolerance requirements on a HLFC wing and investigation of Attachment Line Contamination.

1. INTRODUCTION

Over the last decades, all civil aircraft manufacturers have made great efforts to reduce aircraft drag. The long-term aim of this operation is to reduce the specific consumption of aircraft, which would lead to substantial economic and environmental benefits. A promising technique consists in reducing skin friction drag by delaying the laminar-turbulent transition point as far aft as possible, particularly on the wings, in order to obtain lower friction coefficient in the presence of laminar flow. ONERA scientists have investigated this concept, called "laminarity", for more than three decades (see for instance some recent references [1-8]. In the frame of the HLFC-Win project, funded by the Clean Sky 2 Joint Undertaking under the European Union's Horizon 2020 research and innovation programme, AERNNOVA, DLR, ONERA and SONACA are working jointly with AIRBUS on the development and evaluation of Hybrid Laminar Flow Control technology (HLFC) for large passenger aircraft[1]. More precisely, the target application is a long-range aircraft wing.
Some major aerodynamic challenges that must be tackled to enable the development of HLFC airfoils are: assessment of the wing drag reduction due to HLFC suction; assessment of robustness of advanced suction systems under transonic flow conditions; surface tolerance requirements on a HLFC wing; investigation of Attachment Line Contamination. Within the HLFC-Win project, ONERA is setting-up wind-tunnel investigations for addressing them. Especially, a large-scale HLFC wing model is being prepared for experiments to be conducted at the end of 2022 in ONERA's S1MA wind-tunnel, under transonic conditions (Mach ~ 0.83) and at a high Reynolds number (unitary Re ~ 11.10^6 m^{-1}). In the paper, we present the aerodynamic design of this large-scale wing model and we explain how it will address the challenges listed previously.

2. PRESENTATION OF THE AERO-SHAPE

The high-speed wind-tunnel model was designed starting from an AIRBUS reference airplane shape. The airplane half-span is 29 m roughly. Airfoils suited for HLFC technology were considered only in the outer wing, for spanwise positions over 16 m. The airplane design point corresponds to a Mach number equal to 0.83 and a lift coefficient of 0.50.
Firstly, a parametric study was done to select the model scale and the airplane wing portion to be represented by

[1] Grant agreements No. CS2-GAM-2018-LPA-AMD-807097-38 and CS2-GAM-2020-LPA-AMD-945583-11

the wind-tunnel model. Then a more detailed aerodynamic design was done with high fidelity methods and the so-called ONERA-S1MA shape was selected from this design work. Different computations have been done on this shape to investigate the effects of flow conditions, of boundary layer suction and of the wind-tunnel walls. A variant of this shape with a leading edge sweep angle increased by 20° (ie up to a value of 52°) has also been calculated to analyse the leading edge contamination phenomenon and the associated attachment line transition control.

2.1. Model scale selection

The main objectives of the aerodynamic design of the model are:

- To have during the wind-tunnel tests (WTT) Reynolds numbers as close as possible to flight ones;
- To have contamination in at least 1/3 inner span of model;
- To have in the 2/3 outboard span airfoils suited for HLFC.

In addition, there are several constraints for the model: to have a maximum model span of 4.5 m and a root chord length of 2.0 m roughly, and to have maximum aerodynamic loads acceptable for the wind-tunnel (WT) set-up.

The ratio between the Reynolds numbers expected during the wind-tunnel tests and the airplane flight, as a function of the scale of the WT model, is given in Table 1.

Scale	1.0	1 / 1.772 = 0.564	1 / 2.125 = 0.471	1 / 2.50 = 0.400	1 / 2.765 = 0.362
Re (WTT) / *Re* (flight)	177%	100%	83%	71%	64%

Table 1. Ratio between WTT and flight Reynolds numbers, according to the scale of the wind tunnel model.

A parametric analysis was also done on the leading edge contamination Reynolds number R^*

$$R^* = \left(\frac{W_e}{\nu^*}\right)\sqrt{\frac{\nu^*}{\left.\frac{dU_e}{dx}\right|_{x=0}}} \qquad (1)$$

which is calculated from the leading edge sweep angle, the leading edge radius and from the flow conditions. The kinematic viscosity ν^* is computed at a reference temperature T* which can be estimated from an empirical relationship:

$$T^*=T_e+A(T_w-T_e) + B(T_{aw}-T_e)$$

where T_e is the boundary layer edge temperature, T_w is the wall temperature and T_{aw} is the adiabatic wall (recovery) temperature. $A=0.1$ and $B=0.6$ are empirical constants [9]. The variation of R^* along the span is plotted in Figure 1 for different model scales (colored lines) and compared to what would be obtained for the airplane scale in flight (black line).

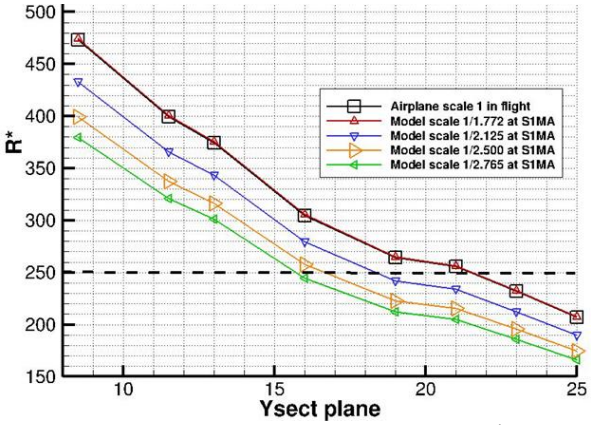

Figure 1. Contamination Reynolds number R^* versus wing span for different model scales

As the objective is here to have contamination in 1/3 inner wing, that is with R^* over 250 [10, 11], and having airfoils suited for HLFC technology in the 2/3 outer wing, that is spanwise positions over 16 m, a model scale of 0.40 was finally selected. With this value, the model will represent the airplane wing portion between spanwise positions 13.50 and 24.75 m (see Figure 2).

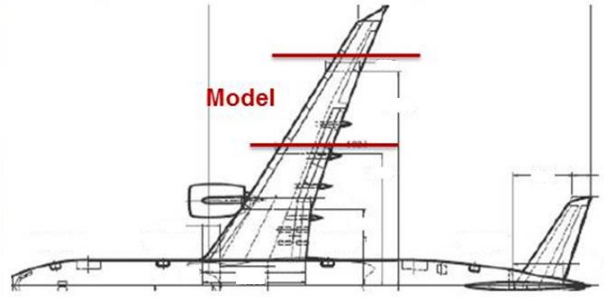

Figure 2. Airplane wing portion corresponding to the S1MA wing model

2.2. Model aerodynamic design

The model aerodynamic design was performed with the elsA software (Airbus-Safran-ONERA property), solving RANS equations [12]. The *k*-ω turbulence model was used for these computations. The transition location predictions were done with criteria integrated in the software: the so-called AHD criterion for

Tollmien-Schlichting instabilities and the so-called C1 criterion for crossflow instabilities [13]. These criteria give only approximate values in case of suction..

The design was done for a Mach number equal to 0.83 and an angle of attack equal to 5.0°. The calculations were done in the S1MA WT conditions, with a Reynolds number equal to 11 millions per meter roughly. An extended laminar flow was desired mainly on the suction side of the wing.
The model design was done without modifying the wing planform, and in particular the leading edge sweep angle was kept equal to 32°. Different geometrical modifications of the initial wing shape were introduced with in-house tools and an analysis of each shape was done with RANS computations:

- Wing global thickness modification;
- Wing twist modifications;
- Airfoil camber modifications;
- Local modifications of the airfoils, in particular to modify the thickness or the leading edge radius.

From the analysis of the different shapes, the so-called ONERA-S1MA shape was selected. It was the best compromise to reach the aerodynamic design objectives. Although the pressure distributions do not fully match with the airplane ones, the shape is not too far from the airplane one and it allows a good similarity for the study of technological aspects, with in particular a suction system and its integration close to what could be done on the airplane. The main geometrical characteristics of this shape are:

- Portion of the airplane wing between spanwise positions 13.50 and 24.75 m;
- Scale 0.40 (1 / 2.50);
- Model span 4.5 m;
- Mean Aerodynamic Chord 1.9658 m;
- Reference surface 8.5976 m^2;
- Wing planform unchanged;
- Wing twist unchanged;
- Airfoils thickness increased by +10%;
- Local modification of the wing tip to have a smooth shape.

3. AERODYNAMIC ASSESSMENT OF ONERA-S1MA SHAPE

Different aerodynamic conditions have been calculated to investigate the model aerodynamic performance, with different angles of attack, and with and without boundary layer suction. The design point is Mach number 0.83 and angle of attack 5.0°. The Reynolds number based on the Mean Aerodynamic Chord is 22 million roughly.

3.1. Variation of angle of attack at Mach number 0.83

The pressure distributions at the design Mach number 0.83 obtained for different angle of attacks are displayed in Figure 3. These computations are performed with boundary layer suction and transition prediction using the criteria. It is applied from position x/c equal to 1.5% on the pressure side of the wing to x/c equal to 20.0% on the suction side. For angles of attack below 4.0°, the suction velocity is equal to 0.3 m/s from 1.5% (pressure side) to 1.5% (suction side), then equal to 0.2 m/s from x/c equal to 1.5% to 5.0% and equal to 0.1 m/s from x/c equal to 5.0% to 20.0%. For angles of attack over 5.0°, a constant suction velocity equal to 0.5 m/s is applied from x/c equal to 1.5% (pressure side) to x/c equal to 20.0% (suction side).
The pressure distributions are typical of the ones observed for a HLFC wing. A strong acceleration is present at the leading edge on the suction side, followed by a region with a decrease of velocities, where boundary layer suction would be applied, and followed by an extended region where the flow is accelerated and where no suction is applied. The extended supersonic region ends with a shock wave, at 80% of the chord roughly. The decrease of velocity in the upstream part of the airfoils allows limited Mach numbers upstream of the shock wave. Nevertheless, the shock wave is quite strong whatever the angle of attack considered, between 2.0° and 6.0°. For angle of attack 6.0° an upstream and weak shock wave is observed, that could be a concern to maintain the boundary layer laminar.

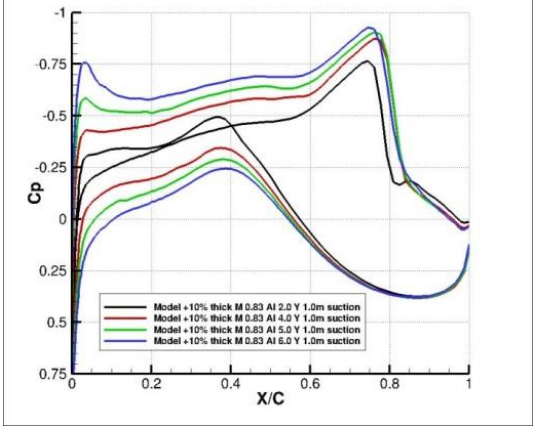

Section Y= 1.0m

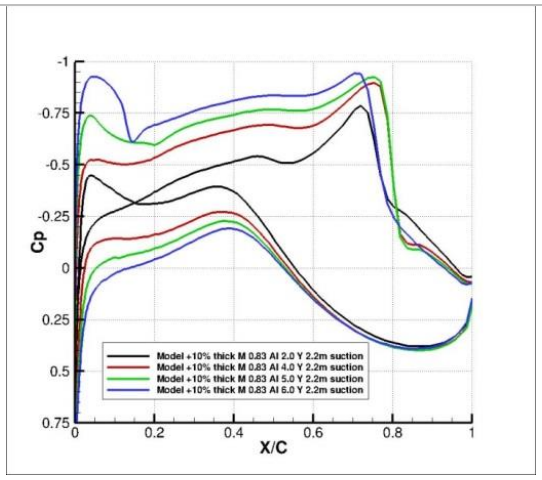

Section Y=2.2m

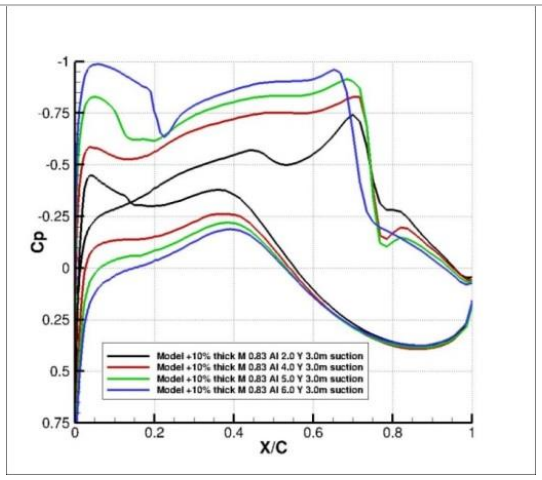

Section Y= 3.0m

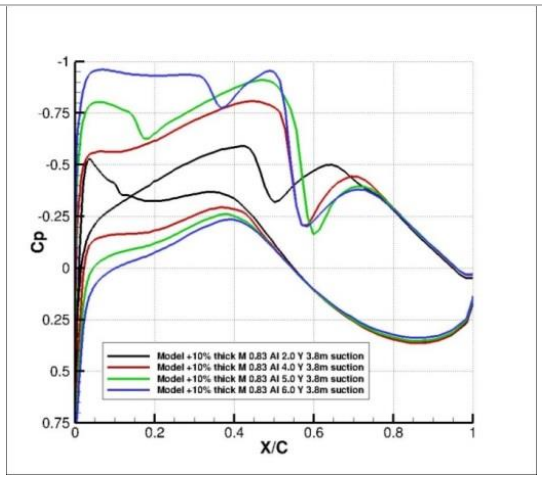

Section Y= 3.8m

Figure 3. Pressure distributions on ONERA-S1MA shape for Mach number 0.83 and different angles of attack: 2.0° (black line), 4.0° (red line), 5.0° (green line) and 6.0° (blue line).

It is possible to evaluate the contamination Reynolds number R^* from the pressure distributions calculated in the region of the stagnation line. Results are shown in Figure 4. For the different angles of attack investigated, the value of R^* is over 250 along the whole span of the wing. It means that the contamination phenomenon is present on the whole wing. For spanwise positions under 1.0 m, ie the region in which contamination phenomenon will be specifically looked at, R^* is higher than 330. R^* is slightly higher for a higher angle of attack.

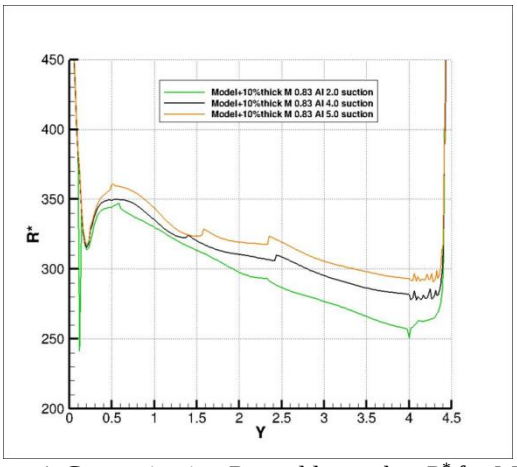

Figure 4. Contamination Reynolds number R^* for Mach number 0.83 and different angles of attack: 2.0° (green line), 4.00 (black line), 5.0° (orange line).

3.2. Influence of wind-tunnel walls

The S1MA test section is very large (approximately 8m of diameter), so even a wing model of this size can easily be placed there, as shown by the sketch in Figure 5 .

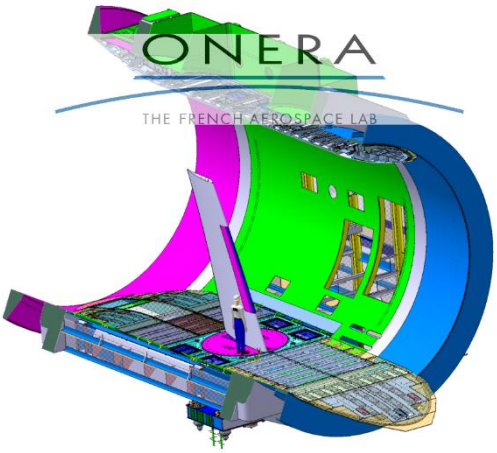

Figure 5. Sketch of the ONERA-S1MA model in the test section.

Several computations have however been performed with the model installed in the S1MA test section in order to investigate the possible influence of the wind-tunnel walls. It should be noticed that these computations overestimate the wind tunnel walls effects because computations are performed with the test section fully closed whereas the tests will be performed with open slots. The slots are longitudinal ones and located at the "corners" of the test section. As a consequence, the computations presented hereafter are indicative only, and show the maximum possible effects due to the wind tunnel walls. During the WTT, the effects created by the walls should be much more reduced.

The installation of the model in the wind tunnel test section creates a blockage effect and it has for consequence an increase of the flow velocities around the model. The isobar lines on the wing suction side, shown in Figure 6, illustrate this phenomenon. For the Mach number 0.83 and the angle of attack 2.0°, an increase of the velocities is observed in the supersonic region on the wing suction side and it has for consequence an increase of the shock wave intensity with a slightly more downstream position. A very slight increase of the velocities is observed on the wing pressure side. Similar tendencies are observed for the Mach number 0.83 and the angle of attack 5.0° but with some differences. On the wing pressure side, the walls effects are of higher intensity than for the angle of attack 2.0°. On the wing suction side, a boundary layer separation is present at the trailing edge and in a large portion of the wing. It generates an upstream displacement of the shock wave that is located upstream of its position without wind tunnel wall at mid span of the wing. Nevertheless, the velocities in the supersonic region remain higher for the case with wind tunnel walls than without wall.

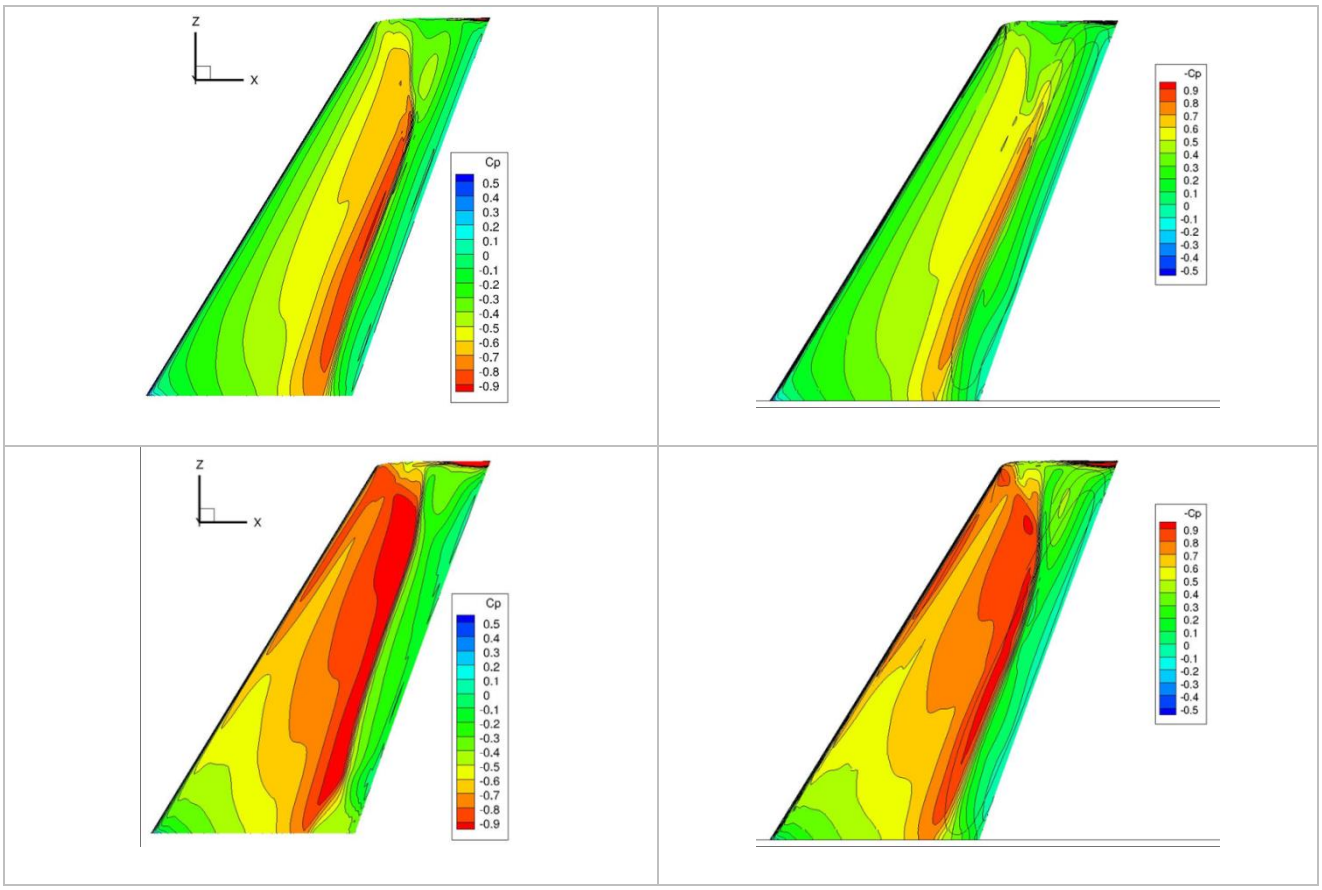

Figure 6. Isobar lines on suction side for Mach number 0.83. Model installed in the S1MA test section (left column) or in free field (right column). Computations obtained foe an angle of attack of 2.0° (upper line) or 5.0° (bottom line).

Different computations have also been performed with a fixed angle of attack of 5.0° and for different Mach numbers, from 0.80 to 0.86. The objective was to determine the flow characteristics when Mach number is increased over the design one, and to investigate possible blockage effects in the wind tunnel. Results are shown in Figure 7.

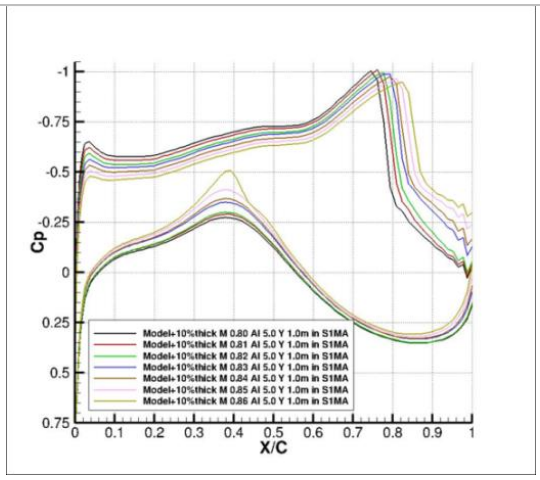

Section Y= 1.0m

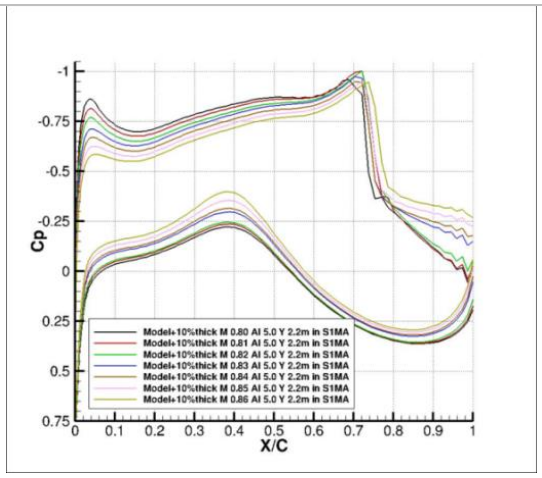

Section Y=2.2m

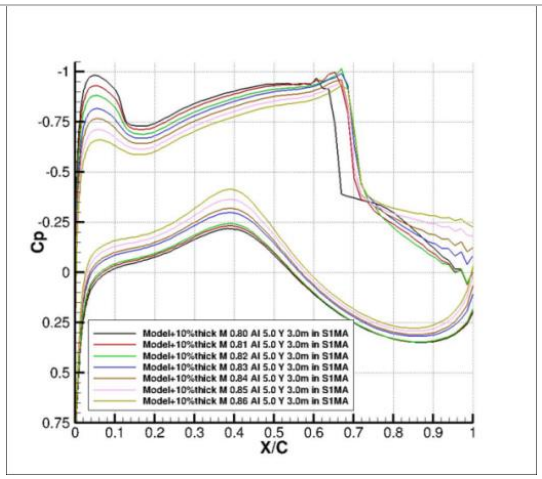

Section Y= 3.0m

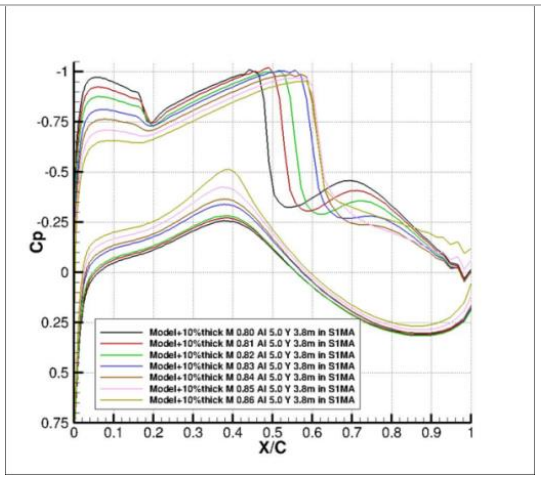

Section Y= 3.8m

Figure 7. Pressure distributions on ONERA-S1MA shape for angle of attack 5.0° and different Mach number increased by 0.01 steps between Mach 0.8 (black line) and Mach 0.86 (yellow line). Model installed in the S1MA test section.

The evolutions of the pressure distributions with Mach number are the usual ones. The shock wave position only slightly changes with Mach number in the central part of the wing. A separation is present at the wing trailing edge for Mach number 0.83 and higher Mach numbers. Nevertheless, as previously said, these computations are done with wind tunnel slots closed and they show a higher intensity of the wind tunnel walls effects in comparison to the conditions for which will be performed the tests, with wind tunnel slots open.

3.3. Influence of increased leading edge sweep

In order to investigate the leading edge contamination phenomenon and to obtain high values of the Reynolds number R*, over 600, it decided that the model should be rotated by 20° during the wind-tunnel tests: the leading edge sweep angle would be changed from 32° to 52°. With such a rotation, the model planform and airfoils remain unchanged.

Different computations of this new shape have been performed, for the Mach number 0.83 and different angles of attack. For the angle of attack of 2.0°, the increase of sweep angle leads to an important modification of the pressure distributions on the model. As expected, the velocities on the wing and especially on the suction side are strongly reduced, and there is no more acceleration of the flow and no more shock wave. Of course these new pressure distributions are no more adapted to hybrid laminar flow control but this configuration will not be tested for this purpose but only for the study of leading edge contamination. Similar phenomena are observed for the Mach number 0.83 and

the angle of attack 5.0°. The flow velocities are reduced when the sweep angle is increased, the flow is no more supersonic on the suction side of the model and there is no more shock wave. On the main part of the wing suction side, the velocities are decreasing along the chord. The isobar lines on the wing suction side, shown in Figure 8, confirm these observations, in particular the disappearance of the supersonic region.

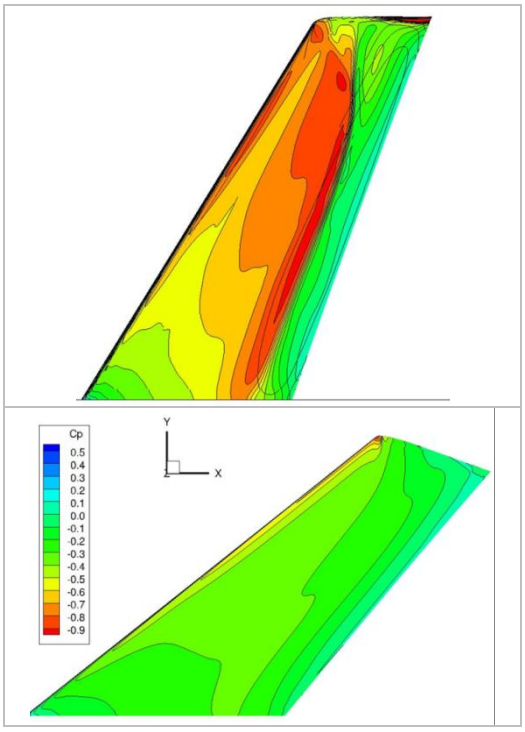

Figure 8. Isobar lines on suction side for models with sweep angles 32° (top) and 52° (bottom). Computations for Mach number 0.83 and angle of attack 5.0°

With this increase of sweep angle, the intensity of the contamination phenomenon is strongly increased. This is illustrated by the values of the contamination Reynolds number R^*, around 300 for the leading edge sweep angle 32° and reaching values over 600 for the sweep angle 52°. The contamination is intense in the inboard part of the wing and decreases along the span. For the sweep angle 52°, the intensity of the phenomenon is nearly the same for the angles of attack 2.0° and 5.0°).

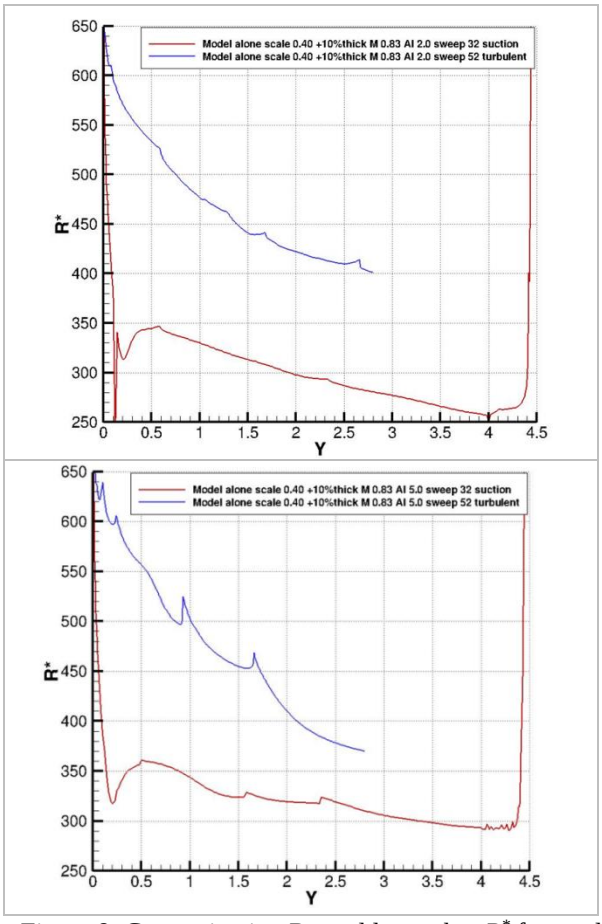

Figure 9. Contamination Reynolds number R^* for model with sweep angle 32° (red line) or 52° (blue line). Computations for Mach number 0.83 and different angles of attack: 2.0° (top) and 5.0° (bottom).

4. ANALYSIS OF THE BOUNDARY-LAYER TRANSITION

Boundary layer computations have been performed using the 3C3D boundary layer code [14]. The boundary layer calculation is fed by the 3D external flow around the wing obtained in the fully turbulent RANS calculations. In order to model the transition onset, the parabola method is used [15]. This method is compatible with the introduction of the suction. The parabola method enables to tackle with both Tollmien-Schlichting (TS) and crossflow (CF) instabilities. As it is an envelop method ($\Psi_{CF,max}$=88.5°, $\Psi_{TS,max}$=40°, Fmax=50000Hz, 100 frequencies), in the S1MA conditions the N threshold value for transition is taken at 8 for both CF and TS instabilities.

The boundary layer suction distribution was specifically adjusted to ensure a maximum laminar extent while being compliant with the flow rate limits of the suction system that will be installed inside the model. Two main configurations have been simulated :

- uniform suction: 0.5 m/s from -1.5% up to 20% chordwise
- variable suction: 0.45m/s from -1.5% up to 0.3% chordwise, suction rate 0.30m/s from 0.3% up to 5% and suction rate 0.15 m/s from 5% up to 20%

In order to have some inputs for an accurate calibration of the N threshold during the wind tunnel tests, an NLF area has been kept on the model. This NLF area will be obtained for a non-nominal flow condition. Thus, the HLFC area extents from 1m up to 3.5m spanwise only.

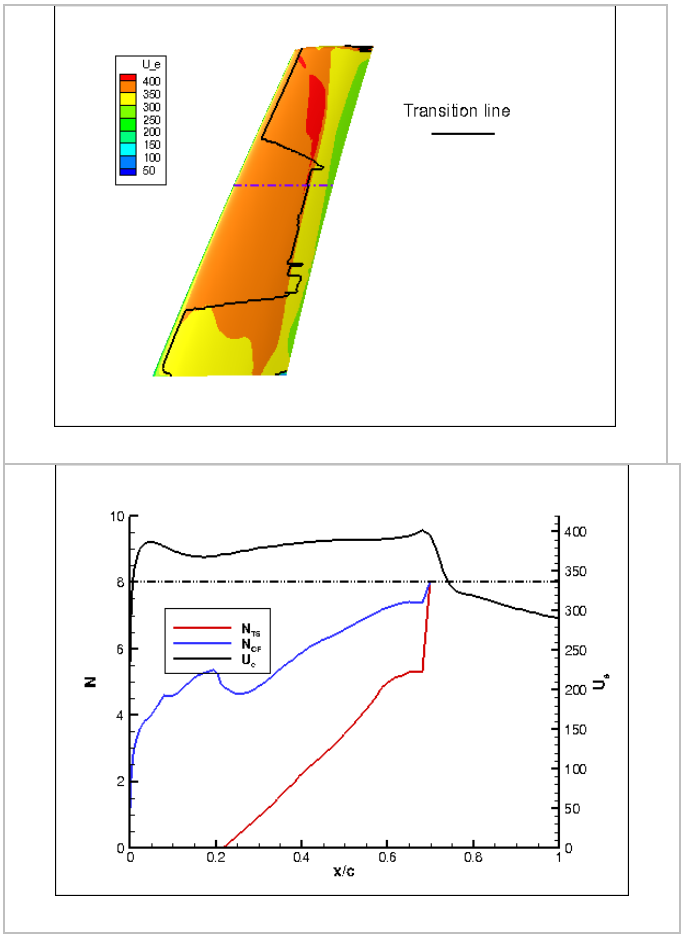

Figure 10. Boundary layer results for Mach number 0.83 and angle of attack 5.0°. Variable suction configuration. Top: Map of the transition on the suction side of the model. Bottom: Plot of the N-factors growth (TS in red, CF in blue) at the spanwise location materialized by the purple line on the transition map figure.

Figure 10 presents the results of the boundary layer transition analysis and highlights that the variable suction configuration enables to have a laminar extent up to the shock location. This configuration has been selected in order to minimize the suction rate. The chordwise change of the suction rate is made possible by the use of suction panels that have a variable porosity, mounted on three suction chambers only in the chordwise direction. The development and the validation of such a simplified suction system is one of the main objectives of the HLFC-Win project. In particular, AERNNOVA is maturating the technology for manufacturing the variable porosity perforated sheets; the S1MA model will be equipped with such panels.

Results presented in Figure 10 also show that with this aerodynamic condition and for this wing design, it is important to suck at a quite high rate close to the leading edge in order to control the CF instabilities since they are the most amplified (compared to the TS instabilities). It must be pointed out that the uniform suction configuration (0.5 m/s on all the suction area) guarantees the same laminar extent. This configuration is therefore considered as a maximum design point in the design activities of the suction piping system inside the model.

5. SURFACE TOLERANCE INVESTIGATION

The ONERA-S1MA model is also designed so that surface tolerance investigation can be performed. There is indeed a lack of experimental data to validate and calibrate the models of allowable surface tolerance at the downstream edge of a suction panel, especially under transonic conditions. Therefore a surface defects device will be installed on the model, as shown in Figure 11.

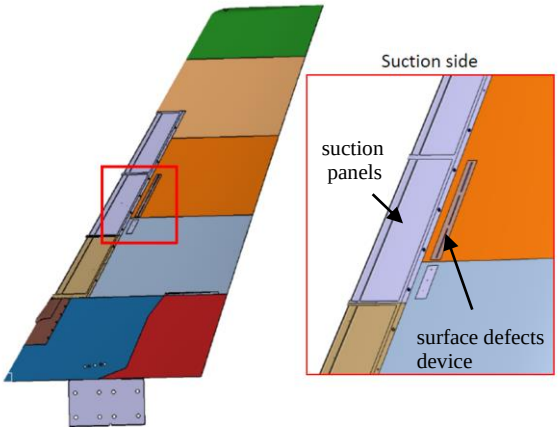

Figure 11. Implantation of the surface defects device

The dimensions of this device were defined according to the results of boundary-layer computations, and with the help of previous results obtained at ONERA on transition triggering by surface defects, even if these ones were limited to subsonic conditions [1, 3]. The

device is located at 25 % chordwise. It will allow to create 3 different gap widths (4.5, 6 and 7.5 mm) and the gap depths range from 0 down to 2.5mm.

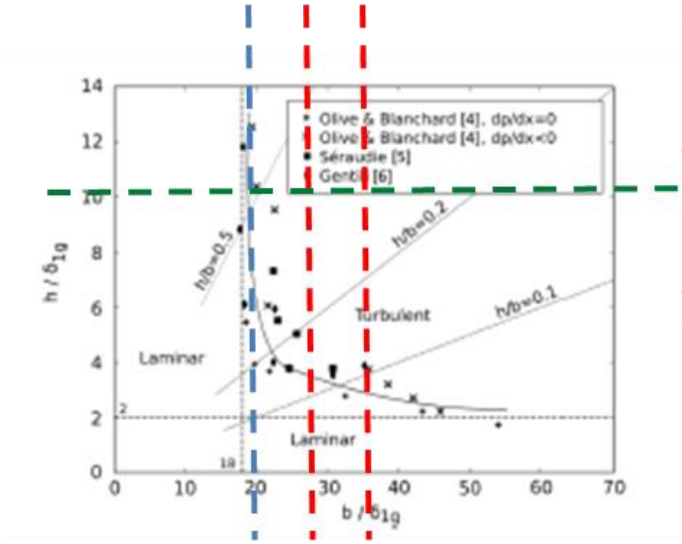

Figure 12. Gap definition based on Beguet et al [3]. The gap depth (*h*) ranges from 0 down to 2.5 mm, the gap width (*b*) is equal to 4.5, 6 or 7.5 mm.

Figure 12 proposes an extract from Beguet et al. paper. The dashed lines correspond to the value of the gap dimensions regarding the boundary layer displacement thickness computed at the target flow conditions in the wind tunnel. Several pins defects will also be created. The dimensions of the surface defects will be automatically changed during the wind tunnel run and so it enables to do some parametric study during the same run. Each device has an actuator and a sensor which enables to accurately control the dimensions achieved by the defect (gap depth or pin height or depth).

6. CONCLUSION

As part of the HLFC-Win project, included in the Large Passenger Aircraft initiative funded by the Clean Sky 2 Joint Undertaking under the European Union's Horizon 2020 research and innovation programme, ONERA is leading the activities devoted to Wind Tunnel Tests. These tests will enable a verification of several aerodynamic assumptions made to develop the HLFC concept for a wing and the associated Ground Based Demonstrator prepared by the HLFC-Win partners, as an enabler to reach TRL4 at the end of the project. ONERA S1MA wind tunnel will be used to test a large-scale wing model representative of the outer part of a long-range aircraft under transonic conditions (Mach ~0.83; unitary Reynolds number~11.10^6 m^{-1}). The aerodynamic design of this model was presented in this paper. This is a wing model of 4.5 meters span with a mean aerodynamic chord of 2 meters. The sweep angle can be changed in order to increase the leading edge Reynolds number achieved by the model, and therefore allow investigation on the leading edge contamination phenomenon, and its control by wall suction. A surface defects device was also designed in order to study surface tolerance downstream of the suction panels. The model is being manufactured by the consortium COMPACT, composed of ARA, IBK and Meca-Ouest. The wind tunnel tests will be performed in the winter 2022/2023.

7. ACKNOWLEDGMENTS

This work was funded by the European Union within the frame of the HLFC-WIN project. This project is part of the Clean Sky 2 Joint Undertaking under the European Union's Horizon 2020 research and innovation programme (Grant agreements CS2-GAM-2018-LPA-AMD-807097-38 and CS2-GAM-2020-LPA-AMD-945583-11).

8. REFERENCES

1. Methel, J., Vermeersch, O., Forte, M & Casalis, G. (2019). An experimental study on the effects of positive surface defects on the laminar-turbulent transition of a sucked boundary layer. *Exp. in Fluids.* 60(94).
2. Hue, D., Vermeersch, O., Duchemin, J., Colin, O. & Tran, D. (2017). Wind Tunnel and CFD investigations focused on transition and performance predictions of laminar wings. *AIAA Journal*. 56(1), 132-145.
3. Beguet, S., Perraud, J., Forte, M. & Brazier, J.-P. (2017) Modeling of transverse gaps effects on boundary-layer transition. *Journal of Aircraft* 54(2), 794-801.
4. Fiore, M., Vermeersch, O., Forte, M., Casalis, G. & François, C. (2016) Characterization of a highly efficient chevron-shaped anti-contamination device *Exp. in Fluids* 57 (4).
5. Forte, M., Piot, E., Vermeersch, O., Casalis, G. & François, C. (2016). Research activities of ONERA on laminar airfoils in the framework of JTI Clean Sky SFWA-ITD: transition control *Greener Aviation*, Bruxelles. 11-13 Oct. 2016
6. Forte, M., Piot, E., Perraud, J.,Hue, D., Duchemin, J. & Vermeersch, O. (2016). Research activities of ONERA on laminar airfoils in the framework of JTI Clean Sky SFWA-ITD: transition prediction. *Greener Aviation*, Bruxelles. 11-13 Oct. 2016
7. Thibert, J.-J., Quast, A., Robert, J.-P. (1992), The A320 Laminar Fin Programme. *1st European Forum on Laminar Flow Technology*, Hamburg, 16-18 March, 1992.

8. Reneaux, J. (2004). Overview on Drag Reduction Technologies for Civil Transport Aircraft, *ECCOMAS 2004 congress*, Jyväskylä, 24-28 July, 2004.

9. D.I.A Poll. (1985). Boundary layer transition on the windward face of space shuttle during re-entry. *AIAA paper 85-0899*.

10. Arnal D. (2004). Laminarity and laminar-turbulent transition control. In *Proc. 3AF 39ème Colloque d'Aérodynamique Appliquée*, Paris, 22-24 March 2004.

11. Poll D.I.A (1978). *Some Aspects of the Flow near a Swept Attachment Line with Particular Reference to Boundary Layer Transition.* Cranfield Inst. of Techn. CoA Report No. 7805.

12. Cambier, L., Heib, S. & Plot, S. (2013) The ONERA elsA CFD software: input from research and feedback from industry, *Mechanics & Industry*, 14(3), 159-174.

13. Cliquet, J., Houdeville, R., & Arnal, D. (2008) Application of Laminar-Turbulent Transition Criteria in Navier-Stokes Computations. *AIAA Journal*. 46 (5). 1182–1190.

14. Houdeville, R. (1992) Three-dimensional boundary layer calculation by a characteristic method. In *Fifth Symposium on Numerical and Physical Aspects of Aerodynamic Flows*. Long Beach. January 1992.

15. Perraud, J. Arnal, D., Casalis, G., Archambaud, J.-P., Donelli, R. (2009). Automatic transition predictions using simplified methods. *AIAA Journal*, 47(11).